

Instrumentation Term Paper

Yifan Zhou

University of Arizona

yifzhou@email.arizona.edu

1. Introduction

Infrared Array Camera is the near infrared imaging instrument equipped on Spitzer Space Telescope. NIRCам is the imaging camera on James Webb Space Telescope (JWST). I listed the general design and performance comparison of these two instrument to illustrate the big leap of NIRCам comparing to IRAC.

Although exoplanet observation is not the key factor in defining the IRAC design, astronomers made great progress in detecting and characterizing exoplanet with the help of IRAC. I listed several key discoveries in exoplanet with IRAC to demonstrate what aspect of IRAC is made use of in exoplanet studies. With the comparison of optical performance, we can see the potential of NIRCам in exoplanet observations.

2. Instrumentation Design

2.1. Optical Design

The optical design of Spitzer IRAC and JWST NIRCам are demonstrated in figure 1.

2.1.1. *IRAC*

The optics path of IRAC is relatively simple comparing to that of NIRC*am*. Two pickoff mirrors that are slightly displaced and tilted separate the light into two beams. Each reflected beam then passes doublet lenses to be reimaged at the focal plane. After the doublet lenses, two Ge substrate beam splitters separate the lower beam into Channel 1 (reflected) and Channel 3 (transmitted) and the upper beam into Channel 2 (reflected) and Channel 4 (transmitted). Finally 4 Channels of light are received by 4 detectors accordingly. This design enables IRAC to take image in 4 different bands simultaneously.

2.1.2. *NIRC*am**

NIRC*am* consists of two modules, each imaging a $2.16' \times 2.16'$ field of view. The modules are built on two optical benches mounted back-to-back. As a result, the two fields of views imaged by the modules are adjacent. The modules are functionally identical, with identical optical and focal plane components. They are mirror images of each other except for coronagraphic pupil masks.

The optical design of each module is shown in figure 1. There are more devices on the optics path of NIRC*am* to enable different observation mode. After reflection of pickoff mirror and first fold mirror, the light are then split by a dichroic beam-splitter into long wave beam and short wave beam. Before the two beams reach the detector, two filter wheels are equipped on the paths so that multi-band imaging can be accomplished. After the pick-off mirror, there is a coronagraph elements to provide NIRC*am* the ability to make coronagraphic measurements.

Several optical elements are added or specially designed for optical accuracy improvement. The pickoff mirror is actuated by a three degree-of- freedom focus and alignment

mechanism that provides fine positioning in tip, tilt, and piston, allowing NIRC*am* to accommodate small pointing and focus changes that may manifest themselves once the Observatory is on-orbit. Internal calibration sources including a flat field source and a coronagraphic source are used to aid with on-orbit calibration and characterization.

2.2. Focal Plane Array

2.2.1. IRAC

IRAC has 4 detector arrays to receive photons in 4 channels. The 4 arrays are all 256×256 pixels in size and have the same physical pixel size of $30 \mu\text{m}$. The channel 1 and channel 2 arrays are made of InSb while the longer wavelength channels 3 and 4 are Si:As detectors.

2.2.2. NIRC*am*

NIRC*am* is based on 2048×2048 HgCdTe photodiode chips, with physical pixel size of $18 \mu\text{m} \times 18 \mu\text{m}$ pixels. The chips used for the short and long wavelength channels are based on different types of HgCdTe. However, in what concerns their functionality and control they are basically identical. The sensitive area of a chip is 2040×2040 pixels, due to a 4 pixel wide border of reference pixels along all edges. Reference pixels are used for tracking bias drifts during an exposure. The finer pixel scale of the short-wavelength channels requires a Focal Plane Array, i.e. a 2×2 mosaic of chips butted with a small gap (5) between them. The resulting gaps in the images have to be filled by dithering moves of the telescope. The long wavelength channels use a single chip. The fields observed by the two modules are adjacent with about $50''$ separation. Also this larger gap in the images has to be filled by dithering moves.

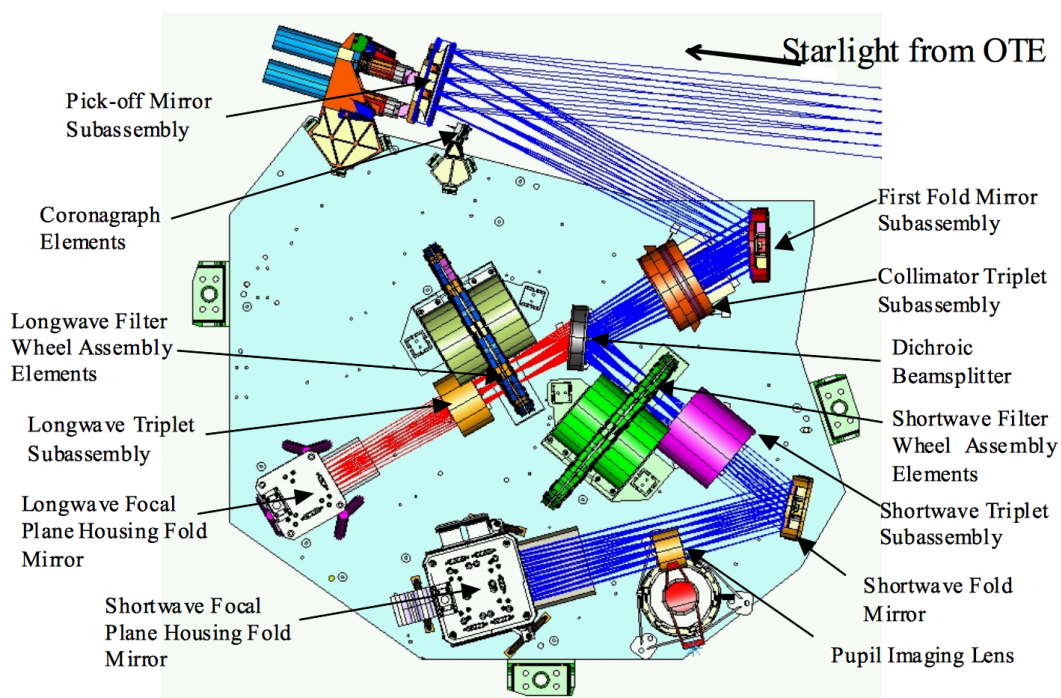
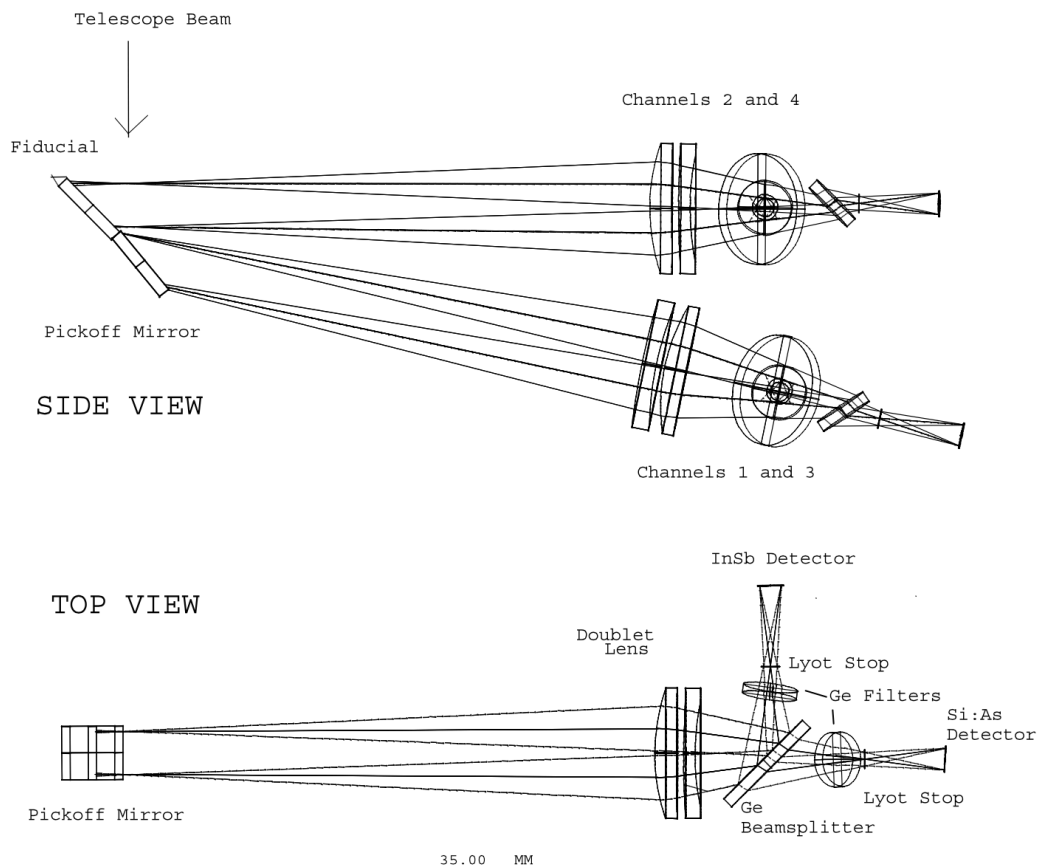


Fig. 1.— Optical Design of Spitzer IRAC (above) and JWST NIRCam (below).

2.3. Operation Mode

2.3.1. *IRAC*

The four 256×256 Focal Plane Arrays can be read out with different operation mode. They are full-array readout mode, stellar photometry mode and subarray mode.

In full-array readout mode, there were four selectable frame times: 2, 12, 30, and 100 s. To allow sensitive observations without losing dynamic range, there was a high dynamic range (HDR) option.

Stellar photometry mode was available for observations of objects much brighter in channels 1 and 2 than in 3 and 4 (typically stars). This mode took short exposures in channels 1 and 2, and long exposures in channels 3 and 4. The sensitivities of each frame are identical to those in full array mode.

For very bright sources, a subarray mode was available. In this mode, only a small 32×32 pixel portion of the array was read out, so the field of view was only $38' \times 38'$. Mapping was not allowed in subarray mode. In subarray readout mode, there were three selectable frame times: 0.02, 0.1, and 0.4 sec. This mode allows observer to catch fast variability of the targets.

2.3.2. *NIRCam*

Comparing to IRAC, NIRCam equipped with much more complicated devices, which allows different observation to be made with.

The primary purpose of the NIRCam instrument is to take image measurement. For imaging observation, the major difference from IRAC is that both short wave and long wave channels of NIRCam are furnished with a Filter Wheel that allows for observations

through more than 12 different spectral bands. There are totally 30 filters on NIRCam, whose wavelength covers from 0.7 to 4.8 μm .

Another unique feature of NIRCam is the ability to make Coronagraphic measurements. In coronagraphic mode, a coronagraphic occulting mask that can be chosen from a selection of sinc^2 , top-hat, and Gaussian designs, optimized for light at either 2.0 or 4.6 μm block the light from the bright sources. This mode is essential in high contrast imaging observation, e.g. direct imaging of exoplanets.

NIRCam is also available for spectroscopic observation. NIRCam has a grism in the long wavelength channel. The grism offers the capability to carry out slitless spectroscopy in the wavelength range 2.4 to 5 μm , with spectroscopic resolution $R \sim 2000$.

3. Instrument Performance

As a detector equipped on the next generation infrared space telescope, NIRCam definitely surpasses IRAC in different ways. Here I compare several key factors that most valued by exoplanet observation between IRAC and NIRCam to illustrate the great potential of NIRCam of expanding our horizon on exoplanet. There factors are spatial resolution, spectral coverage, sensitivity, dynamic range and frame rate.

3.1. Spatial Resolution

High spatial resolution is essential in direct imaging observation. Limited by small primary mirror size of Spitzer Space Telescope (0.85 m), it is not IRAC's strength to spatially resolved objects. The FWHM of point spread function (PSF) is $1''.66, 1''.72, 1''.88$ and $1''.92$ at 3.6, 4.5, 5.8 and 8.0 μm channels, which is high for direct imaging study. The large pixel

scale ($1''.2$) resulting in under sampled PSF makes the situation even worse. As a result, IRAC is hardly ever used for imaging of wide orbit planetary mass companions.

The 6.5 m sized primary mirror of JWST provide NIRCam with significant spatial resolve ability. NIRCam’s PSF has FWHM of $0''.063$, and is nearly 20 times sharper than that of IRAC. The pixel scale that is optimized at $2\ \mu\text{m}$ ensured well sampled PSFs at that wavelength. At smaller wavelength, the PSF would be a little undersampled. However the sample rate is still better than IRAC.

3.2. Wavelength Coverage

IRAC covers four wavelength channel at 3.6, 4.5, 5.8 and $8.0\ \mu\text{m}$. The wavelength coverage of NIRCam which ranges from 1 to $5\ \mu\text{m}$ lacks long wave length ability comparing to IRAC. However, more than 30 filters supplied with NIRCam would provide spectral energy distribution with fine structures.

3.3. Sensitivity

Low thermal emission of exoplanets call for high sensitivity. Table 1 and figure ?? illustrate the sensitivities of IRAC and NIRCam. In figure ??, sensitivities are expressed as the flux required to get $10\ \sigma$ signal with a 10000 s exposure. Since $\sigma \sim \sqrt{t}$, $10\ \sigma$ signal with 10000s exposure is generally equivalent to $1\ \sigma$ signal with 100s exposure. Comparing to IRAC, NIRCam is more than 30 times sensible with wide band filter and more than 10 times sensible with narrow band filter.

Table 1. IRAC Sensitivity (1σ , μJy), citeFazio 2004

Frame Time (s)	$3.6\mu\text{m}$	$4.5\mu\text{m}$	$5.8\mu\text{m}$	$8.0\mu\text{m}$
200	0.40	0.84	5.5	6.9
100	0.60	1.2	8.0	9.8
30	1.4	2.4	16	18
12	3.3	4.8	27	29
2	32	38	150	92
0.6	180	210	630	250
0.4	86	75	270	140
0.510	470	910	420	
0.02	7700	7200	11000	4900

4. Application in Exoplanet

Initially, the most important in defining the IRAC design was the study of the early universe (citeFazio 2014). However, with the advantage in infrared wavelength coverage and high sensitivity, IRAC plays a great role in exoplanet observation. Although IRAC is limited by its design, e.g. the large FWHM of PSF is an obstacle for IRAC to carry out direct imaging of exoplanet, IRAC is the best devices for infrared transiting photometry before the launch of JWST.

Exoplanets' low surface temperatures locate their thermal emission peaks in infrared. Specially hot Jupiters whose effective temperatures are about 1000 K, are most ideal targets to detect thermal emission with. citeCharbonneau 2005 took advantage of IRAC's high photometry precision to first detect the secondary eclipse of exoplanet TrES-1 which confirmed the thermal emission coming from the planet. They observed the target two channels, (4.5 and 8.0 μm), observed the field, and obtained 1518 full-array images in each of the two band-passes citeCharbonneau. The great accuracy of spitzer photometry data made it possible for them to construct the light curve presented in figure 2 and detect the secondary eclipse dip.

In subarray mode, the high read out speed of IRAC is utilized to monitor the temporal variability of exoplanet. citeKnutson 2007 observed HD189733 that is an eclipse planetary system containing a hot Jupiter and constructed a map of the distribution of temperatures by modeling the variability of the light curve. They monitored HD 189733 continuously over a 33.1 hour period using the 8 μm channel of IRAC in subarray mode with a cadence of 0.4 s. With the high cadence, high precision time series data (3), they saw a distinct rise in flux beginning shortly after the end of the transit and continuing until a time just prior to the beginning of the secondary eclipse, from which they created the map of exoplanet temperatures.

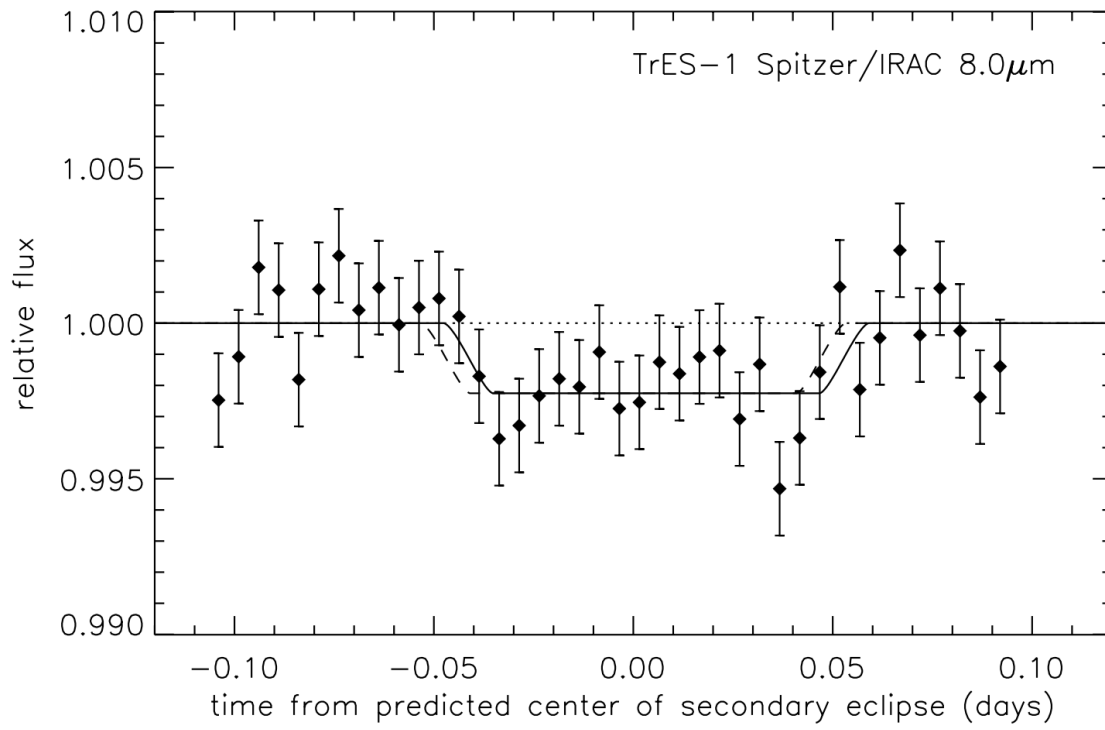


Fig. 2.— Light curve of TrES observed by IRAC Channel 4 ($8\mu\text{m}$) citeCharbonneau 2005.

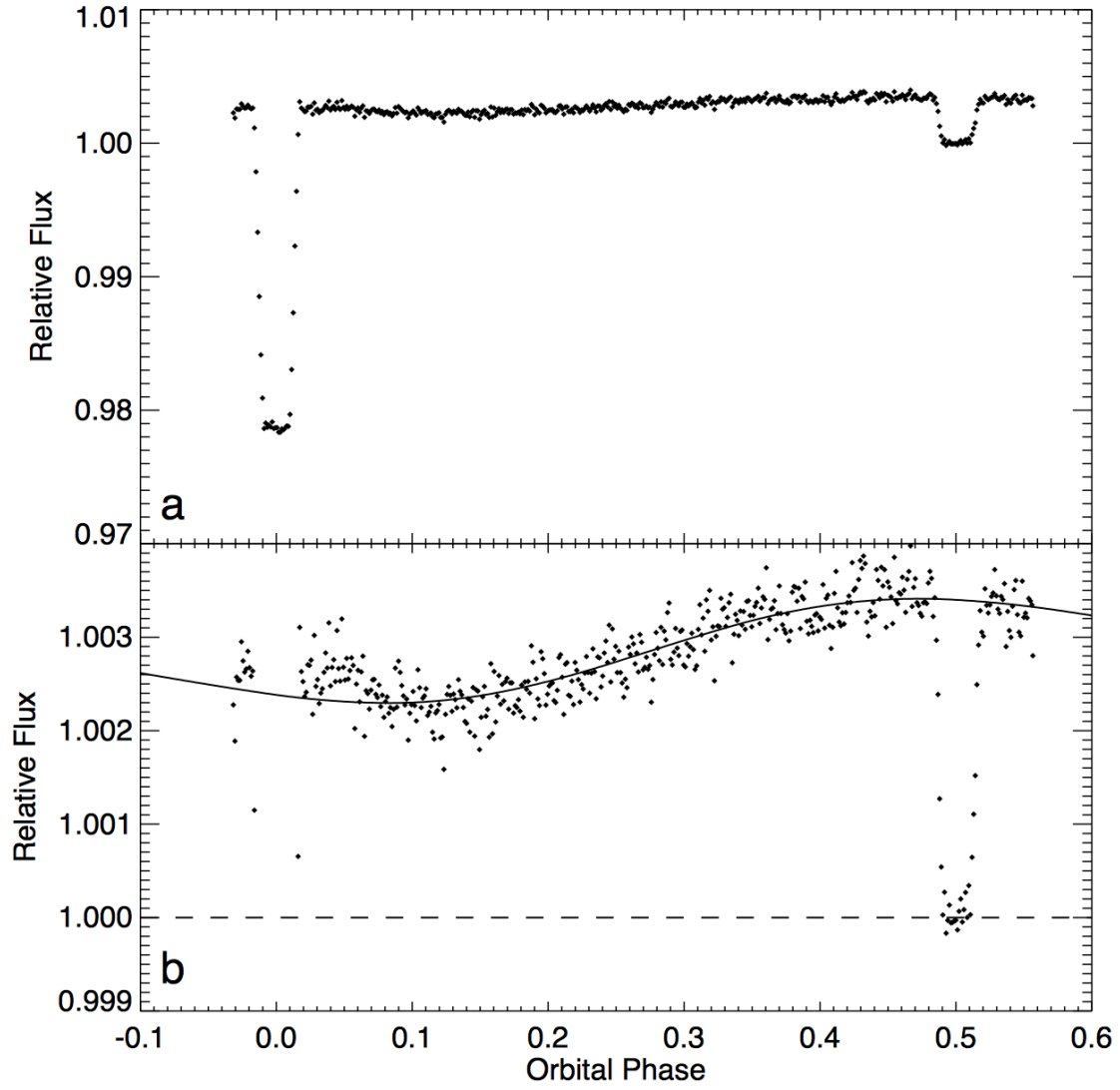


Fig. 3.— Light curve of high cadence observation of HD189733 system

The combination of 4 channel photometries of IRAC could open a window for the study of exoplanet atmosphere citeBurrows 2014. By comparing multi-band eclipse/secondary eclipse photometry with model spectrum, water and dust cloud feature can be traced citeO’Donovan 2010.

5. Summary